Von Herzen, R. P., Robinson, P. T., et al., 1991
Proceedings of the Ocean Drilling Program, Scientific Results, Vol. 118

18. ELECTRICAL CONDUCTION IN OCEANIC GABBROS, HOLE 735B, SOUTHWEST INDIAN RIDGE[1]

Philippe A. Pezard,[2,3] James J. Howard,[4] and David Goldberg[2]

ABSTRACT

The resistivity, porosity, and cation exchange capacity of 29 gabbroic samples recovered in Hole 735B during Leg 118 of the Ocean Drilling Program (ODP) were measured in the laboratory at room temperature and atmospheric pressure. The samples of lithologic Units IV and VI containing iron and titanium oxides have the highest electrical conductivity and the largest grain density sampled in Hole 735B. The fresh samples are the most resistive of the data set, and the tectonized samples (either due to plastic or brittle deformation) have intermediate values.

Cation exchange capacity and electrical resistivity measurements performed at four different fluid salinities indicate that surface conduction mechanisms can be ignored for *in-situ* measurements of electrical resistivity at Site 735. The main conduction mechanisms for electrical current consequently are reduced to (1) electrolytic conduction in the pore space and (2) electronic conduction in metallic grains of the matrix in the presence of Fe-Ti oxides. In the last case, matrix conduction might become the dominant conduction mechanism, which explains the low resistivity values recorded *in situ* with the dual laterolog in lithologic Unit IV and in the lower part of the hole. The conduction equation is then written as follows:

$$C_o = [(C_w/\mathrm{FF}) + C_{\mathrm{oxides}}],$$

and the low m value obtained when relating porosity to formation factor with

$$\mathrm{FF} = (8.04)\ \phi^{-1.08},$$

which suggests that the conducting pore space of gabbros is similar to that of mid-ocean ridge basalts (MORB), that is, mainly constituted of cracks and microcracks, as elsewhere observed in thin sections.

INTRODUCTION

The study of the physical structure of oceanic plates has been a subject of widespread interest in geosciences for the past 50 yr, particularly since the advent of plate tectonics in the 1960s. Several DSDP/ODP drilling campaigns (Anderson, Honnorez, Becker, et al., 1985; Donnelly, Francheteau, et al., 1979; and many others) succeeded in penetrating the upper oceanic crust, often as deep as a kilometer, both in young crust near mid-ocean ridges (DSDP Holes 395A and 504B) and in abyssal plains (DSDP Holes 417A, 417D, and 418A). In that context, the most remarkable achievement to date remains DSDP/ODP Hole 504B, where a 600-m-thick dike complex was drilled, thus confirming the similitude between the structure of oceanic plates and that of ophiolites. However, Hole 504B is still at least 500 m short of layer 3, as indicated by a vertical seismic experiment (Becker, Sakai, et al., 1988). Besides short intervals of peridotites recovered from continental margins (Boillot, Winterer, et al., 1987), international efforts to sample continuously the gabbros of layer 3 or oceanic mantle rocks failed until Leg 118. Consequently, Hole 735B provides for the first time a window into the lower oceanic crust and thus the opportunity to study the physical properties of oceanic gabbros. In particular, porosity and permeability data are important to the study of the hydrological budget of the crust.

Unlike bulk density, acoustic velocity, or electrical resistivity, *in-situ* measurements of porosity of the oceanic basement are not at present directly measurable using geophysical logs. Whereas porosity is estimated routinely from resistivity (Archie, 1942), nuclear (Ellis, 1987), or acoustic (Wyllie and Gregory, 1953) experiments in sedimentary formations, the very different strucure of the pore space of crystalline rocks, or the presence as traces of elements such as gadolinium or boron (with large capture cross sections to neutrons), has prevented to date the development of an accurate method for deriving porosity in basement from *in-situ* geophysical measurements. The gabbros recovered in Hole 735B provide an even more complex situation with the presence of conductive iron and titanium oxides (Robinson, Von Herzen, et al., 1989). In this case, matrix conduction mechanisms might become as important as electrolytic or cationitic mechanisms (Pezard, in press), or even dominant, as reported by Drury and Hyndman (1979) for dry oceanic basalts, as metallic oxide grains were observed to be the prime electrical conductor.

The extreme sensitivity of electrical properties to a large number of parameters in fact makes electromagnetic methods a complex and powerful technique for studying large- and small-scale structures of rock formations. Although the known electrical properties of rocks and minerals have been observed to vary more than 24 orders of magnitude in the Earth (Olhoeft, 1981), the measurements performed so far in oceanic crust have covered less than six orders of magnitude. In that respect, *in-situ* measurements of electrical resistivity respond directly to conductivity changes in the rock surrounding the borehole. The presence of conductive metallic grains such as Fe-Ti oxides in the matrix, or vesicular pores, cracks, and microcracks, either fluid-filled or plugged with precipitated conductive minerals (such as smectites) creates a path

---

[1] Von Herzen, R., Robinson, P. T., et al., 1991. *Proc. ODP, Sci. Results*, 118: College Station, TX U.S.A. (Ocean Drilling Program).

[2] Borehole Research Group of the Lamont-Doherty Geological Observatory, Palisades, NY 10964.

[3] Department of Geological Sciences of Columbia University, NY.

[4] Schlumberger-Doll Research, Old Quarry Road, Ridgefield, CT 06877.

for current flow. The electrical conduction is consequently a combination of electrolytic mechanism for the pore space and the fluid-filled fractures, surface-mediated ion transport mechanism for conductive minerals, and electronic transport for the metallic part of the matrix.

Here, a series of laboratory measurements is reported to evaluate whether the presence of either (1) alteration minerals or (2) Fe-Ti oxides constitutes a significant contribution to current conduction during resistivity logging. This would cause, for example, estimates of porosity using Archie's law to be too high. The results of this experimental analysis are discussed in terms of electrical conduction mechanisms active during *in-situ* experiments and are used to constrain the structure of the conductive pore space in oceanic gabbros.

OPERATIONS IN HOLE 735B

During Leg 118, *JOIDES Resolution* sailed to the Indian Ocean to drill crustal rocks near the Southwest Indian Ridge, in the vicinity of the Atlantis II Fracture Zone. This fracture zone is one of a series of north-south trending transform faults offsetting the slow-spreading Southwest Indian Ridge (Fig. 1). Site 735 is located to the east of the Atlantis II transform, on a narrow platform lying in about 700 m of water. The position of the platform in the magnetic anomaly pattern on the east transform wall suggests a crustal age of about 12 Ma (Robinson, Von Herzen, et al., 1989). A total of 500.7 m were drilled; 434.8 m of olivine gabbro, olivine-bearing gabbro, pyroxene gabbro, Fe-Ti oxide gabbro, troctolite, and microgabbro with rare basalt and trondhjemite were collected in the core. Recovery thus was excellent, with an average of 87%. In addition, an extensive suite of *in-situ* measurements was conducted over the entire length of this drill hole.

LITHOSTRATIGRAPHIC SEQUENCE

In all, six major lithologic units were recognized in the penetrated sequence, with rocks having undergone varying degrees of plastic and brittle deformation (Robinson, Von Herzen, et al., 1989). Figure 2 depicts a series of continuous *in-situ* measurements recorded in Hole 735B, including resistivity, vertical magnetic field, silica, and photoelectric effect. These measurements illustrate the six different lithology units described in the core. Unit I is a 37.4-m-thick sequence of foliated metagabbro with porphyroclastic to mylonitic textures. The igneous textures have been completely destroyed, and a few Fe-Ti oxide-rich layers were observed. Unit II consists of 132.8 m of olivine and olivine-bearing gabbro. Unit III is a 53.4-m-thick sequence of olivine gabbro with a few intervals of Fe-Ti oxide gabbro. A well-developed igneous lamination dips steeply in the upper part of the unit, but flattens with depth, and mylonitic or foliated zones are common. Unit IV is made up of 50.5 m of Fe-Ti oxide-rich gabbro. These gabbros have more abundant opaque minerals (10% or more) and less olivine than those of Unit III. Iron-oxide contents can be as high as 30 wt%, and titanium-oxide contents as high as 9 wt%. A felsic intrusion breccia with trondhjemite veins occurs at two levels within the unit. Unit V consists of 108.3 m of relatively uniform olivine gabbro characterized by a scarcity of Fe-Ti oxides, and low-calcium pyroxenes similar to those of Unit II. Thin troctolite layers and several plagioclase-rich zones are present. Unit VI is a 118.3-m-thick interval of olivine-rich gabbro with frequent layers of troctolite. These gabbros are similar to those of Unit V, but are enriched in olivine. The troctolite and troctolite-gabbros are interlayered with the olivine-gabbros and have been interpreted as small dikes or intrusive layers. These are the most mafic rocks encountered in Hole 735B. A few coarse-grained Fe-Ti oxide-rich gabbros also are present.

CORE MEASUREMENTS

A total of 29 gabbroic minicores were sampled during Leg 118 to measure porosity, grain density, electrical resistivity at four different saturating-fluid salinities, and cation exchange

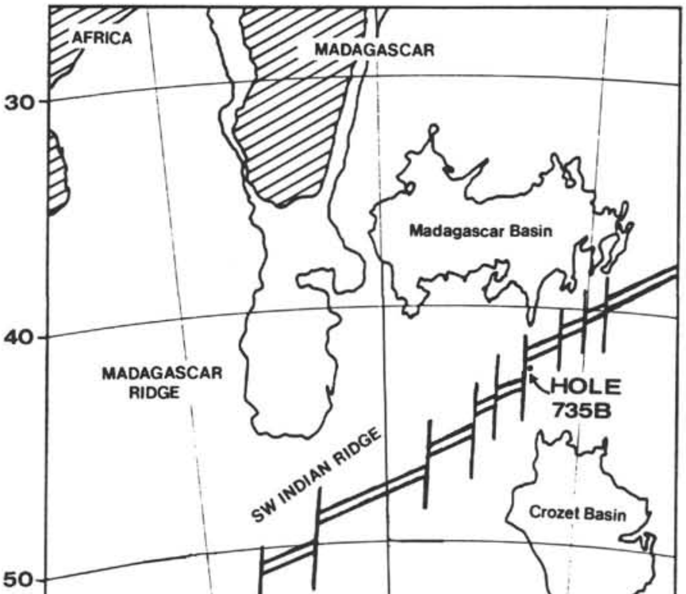

Figure 1. Location map of the drill site on the Southwest Indian Ridge.

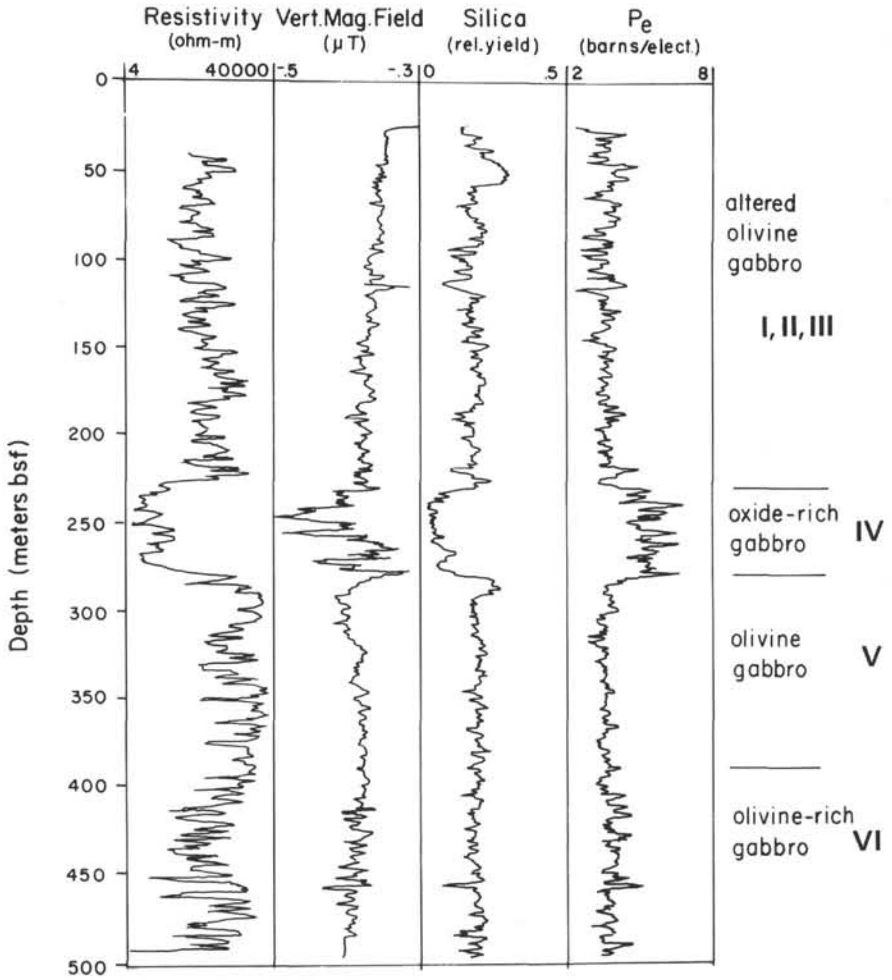

Figure 2. Selected logs in Hole 735B, drilled in layer 3 gabbros. Unit IV, for example, correlates to low electrical resistivity, variable magnetic field, low silica content, and high photoelectric effect (P_e), which indicates a high concentration of conductive Fe-Ti oxides.

capacity (CEC). Minicores were cut from the core on board the ship and immediately stored in seawater to prevent desaturation. Before measuring the resistivity, the samples were saturated with distilled water to eliminate the salts present in the pore spaces. Subsequently, the samples were dried for weight measurements, then saturated under near-vacuum conditions with a 0.195 ohm-m NaCl solution. During the measurements, the samples were kept saturated, and the bath was regularly checked for constant salinity. The 29 samples were selected from each of the six lithologic units (Table 1) and classified for simplicity of reporting into three categories: fresh, tectonized, and Fe-Ti oxide-rich.

Cation Exchange Capacity

The measurement of CEC is often used in oil and gas exploration to evaluate the shaliness of a sedimentary formation (Waxman and Smits, 1968). The objective of this electrochemical analysis is to count the number of cations that might contribute to the conduction of current during an electromagnetic experiment. As smectites are characterized by large CEC numbers (Serra, 1984; Ellis, 1987), the contribution of saponites (present as alteration phases of MORB in Hole 504B) to *in-situ* electrical conduction was documented by Pezard (in press) in a study similar to this one. A standard technique for measuring the CEC of rocks called the Kjeldahl method was described by Ridge (1983). A cation not native to the rock is first fixed on the exchangeable clay sites, then the fixed cations are deliberately removed and their quantity measured.

A small amount of material for each of the 29 samples was crushed, and a quantity of 1 to 2 g was selected after thorough mixing. The samples were made water-wet to disperse the clays, then washed and centrifuged three times with ammonium acetate to locate an ammonium ion at each of the potential exchangeable sites. Once diluted with water and ethyl alcohol, sodium hydroxide was used to replace the ammonium ions. Finally, the ammonium ions were condensed in a reducing environment, collected as ammonia, and titrated in the Kejdahl unit with hydrochloric acid. The results are expressed in milli-equivalents per 100 g of wet rock (meq/100 g), or in milli-equivalents per liter (meq/L), if converted into a CEC per unit pore volume, Q_v (Clavier et al., 1977). Laboratory tests on standards indicate that this technique has a precision of 0.1 meq/100 g, and a sensitivity of the order of 0.5 meq/100 g.

Porosity, Grain Density, and Electrical Resistivity

Porosity and electrical resistivity were measured on the 29 minicores of gabbro, each of which was 25 mm in diameter and 18 to 23 mm long. The samples were cut from the

Table 1. Resistivity (at four different saturating-fluid salinities), porosity, grain density, and CEC of 29 samples.

Sample	Depth (mbsf)	Lithologic unit	Core, section (118-735B-)	Sample	Porosity (ϕ)	Grain density	CEC	Res (0.052)	Res (0.195)	Res (0.502)	Res (1.020)	FF	$B \cdot Q_v$ (μ=10.0)
1	20.00	I	06-1	Fresh	0.011	2.91	4.8	52.9	238.1	322.6	344.8	1017.5	0.452
2	40.00	I	12-1	Tectonized	0.029	2.83	1.2	20.5	67.6	109.9	119.8	394.4	0.040
3	52.45	II	14-2	Tectonized	0.017	3.00	1.2	44.5	163.9	222.2	238.3	855.6	0.072
4	98.87	II	22-4	Tectonized	0.028	2.95	1.1	23.1	61.2	102.6	113.8	444.7	0.040
5	142.98	II	30-5	Fresh	0.007	2.99	5.8	89.0	370.4	607.2	714.3	1710.8	0.548
6	146.43	II	31-3	Fresh	0.010	3.00	4.0	60.5	322.6	581.7	666.7	1164.0	0.400
7	152.31	II	32-4	Tectonized	0.014	2.79	4.2	42.1	147.1	204.1	219.4	809.6	0.286
8	191.45	III	40-1	Fresh	0.011	2.93	2.6	52.0	158.7	294.1	319.5	999.7	0.229
9	201.36	III	41-4	Fresh	0.007	2.99	1.2	76.3	303.0	492.6	545.8	1467.1	0.185
10	225.00	IV	47-3	Fresh	0.008	3.01	2.8	62.2	322.6	485.4	534.2	1195.8	0.348
11	231.93	IV	48-1	Fe-Ti oxides	0.011	3.24	2.3	8.8	12.6	14.0	14.5	168.4	0.245
12	242.81	IV	50-4	Fe-Ti oxides	0.005	3.17	1.9	15.1	23.3	26.2	28.0	290.8	0.412
13	254.86	IV	53-2	Fe-Ti oxides	0.008	3.20	2.6	22.8	38.0	49.8	52.2	438.1	0.375
14	257.83	IV	53-4	Tectonized	0.018	2.95	3.7	30.2	101.6	140.8	153.3	581.2	0.205
15	272.37	IV	56-2	Fe-Ti oxides	0.009	3.26	2.2	10.6	17.5	22.9	24.5	203.8	0.289
16	279.59	V	57-4	Tectonized	0.045	2.87	5.4	12.5	45.2	68.0	75.9	240.3	0.114
17	281.96	V	58-2	Fresh	0.009	3.00	2.3	59.1	309.2	555.6	645.2	1136.5	0.259
18	300.77	V	61-4	Fresh	0.014	2.90	2.5	36.8	157.5	322.6	424.4	707.7	0.181
19	306.43	V	63-1	Tectonized	0.029	2.89	2.8	23.1	75.8	119.0	141.6	443.8	0.096
20	363.86	V	72-5	Fresh	0.007	3.00	1.4	78.7	378.0	571.4	646.6	1513.6	0.221
21	371.41	V	73-5	Fresh	0.009	2.99	1.5	61.7	322.6	540.5	611.3	1187.2	0.165
22	407.83	VI	77-3	Fresh	0.008	2.95	2.2	81.5	435.1	628.9	714.3	1567.7	0.285
23	411.68	VI	78-2	Tectonized	0.031	2.91	2.6	17.9	72.5	91.7	101.8	344.7	0.084
24	420.48	VI	79-5	Fe-Ti oxides	0.008	3.18	3.0	6.1	10.9	12.6	13.8	118.0	0.430
25	432.85	VI	80-7	Fe-Ti oxides	0.007	3.26	2.6	7.4	9.8	10.2	10.5	141.9	0.430
26	477.76	VI	85-5	Tectonized	0.033	2.94	3.0	18.7	64.4	98.3	104.2	360.6	0.090
27	488.25	VI	86-5	Fresh	0.009	2.88	1.4	56.3	243.3	429.5	505.0	1083.3	0.156
28	488.43	VI	86-6	Fresh	0.011	2.81	3.7	47.3	224.9	390.3	483.5	909.8	0.326
29	491.38	VI	87-1	Fe-Ti oxides	0.012	3.28	2.8	11.9	21.8	22.6	23.3	228.6	0.274

CEC = cation exchange capacity; FF = formation factor; Res = resistivity.

working-half of the cores recovered from Hole 735B, perpendicular to the axis of the original core. Electrical resistivities were measured along the axis of the minicores, and thus are representative of the "horizontal" resistivity of the bulk rock.

Porosity was determined by standard immersion methods. The core plugs were saturated with distilled water in an evacuation cell for 48 hr. For dry weights, the plugs were dried at 65°C for 12 hr, then placed at near-vacuum conditions. Because the instrument resolution is ±0.000 1 g and the reproducibility is ±0.0005 g, an experimental error for porosity of ±0.10% (20% of the absolute value for the less porous samples) is inherent to this technique. The electrical resistivity of the samples was measured at 24.5°C and atmospheric pressure, after being saturated again with a 0.195 ohm-m NaCl solution. A 10-mV, 50-Hz signal was applied to the samples with a Wayne-Kerr bridge for measuring at a frequency similar to those used *in-situ* by the dual laterolog. Resistivity was measured with a two-electrode device (Brace et al., 1965; Rai and Manghnani, 1981; Pezard, in press) by attaching stainless-steel electrodes to both ends of each core plug. A teflon wrapping was applied to the cylinder surfaces to prevent desaturation while measuring. Although the instrumental error for resistivity measurements is about 1%, the overall error was as high as 5% because of the difficulty in achieving a reproducible contact between the samples and the steel electrodes.

RESULTS AND DISCUSSION

The results of the physical and chemical properties measured in samples from Hole 735B are summarized in Table 1 and in Figure 3. A crossplot of grain density vs. electrical resistivity provides a definition of the three categories previously chosen to distinguish alteration (Fig. 3). The Fe-Ti oxide-rich samples are the most conductive and have the largest grain densities. As expected, the fresh samples are the most resistive, and tectonized samples have intermediate resistivity values (Fig. 3). A plot of grain density, porosity, resistivity, and CEC as a function of depth is presented in Figure 4. Porosity values are on the order of 1.0% for fresh and oxide-rich samples and 3.0% for tectonized samples. The oxide-rich samples from Units IV and VI cannot be distinguished on the basis of these measured properties.

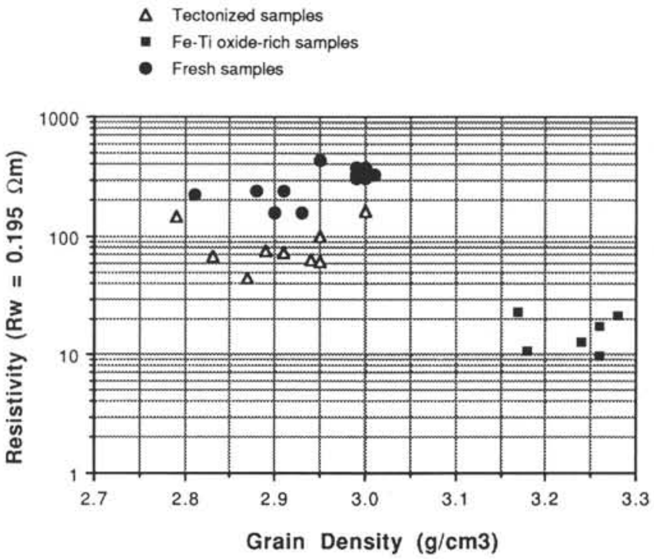

Figure 3. Grain density vs. resistivity (measured with seawater as saturating fluid).

CEC measurements do not follow the same classification-scheme defined by the electrical-resistivity or grain-density crossplot (Fig. 3). Although the CEC does not show any correlation with resistivity (Fig. 5), the contribution of surface

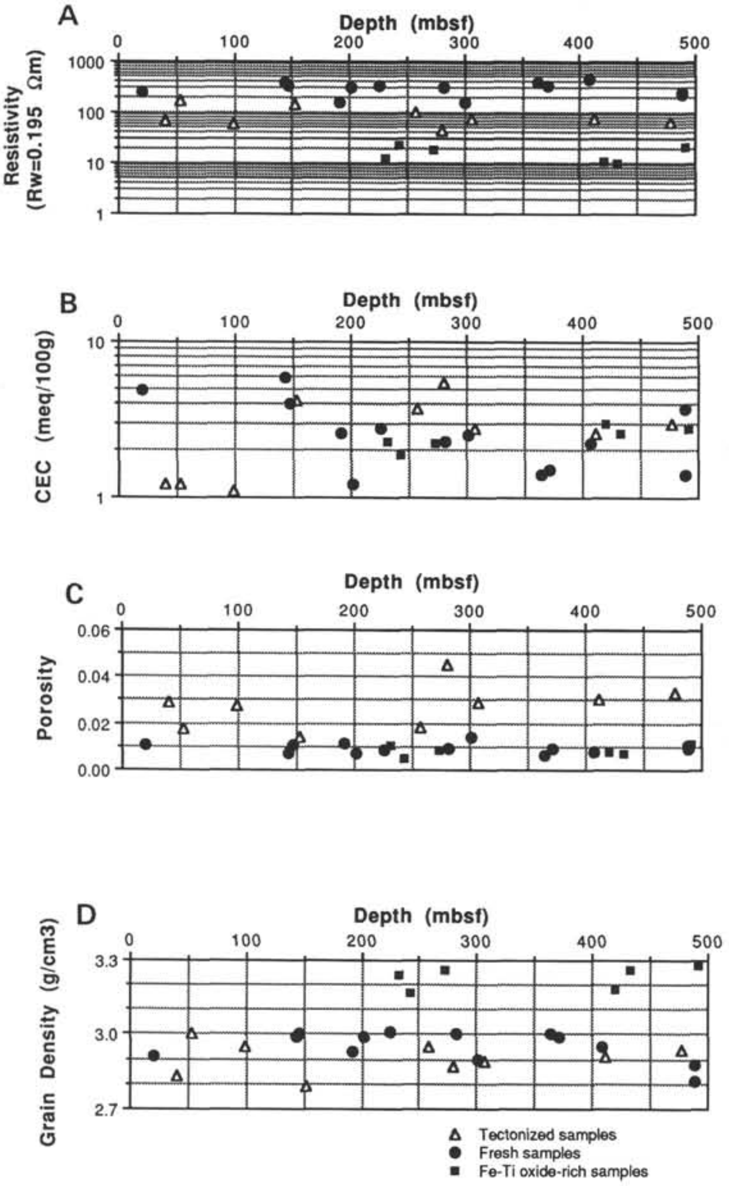

Figure 4. **A.** Resistivity (at seawater salinity); **B.** CEC; **C.** Porosity; **D.** Grain density; vs. depth.

conduction ($B \cdot Q_v/\mu^2$) appears to be nearly constant, regardless of sample resistivity (Fig. 6). An exception to this is constituted by a few tectonized samples having low CEC values in the upper part of Hole 735B (Units I and II; Fig. 4A). The surface conduction contribution was computed according to the model of parallel conduction between pore volumes and pore surfaces (Pezard, in press). This is described by

$$FF = [C_w + (B \cdot Q_v/\mu^2)]/C_o,$$

where FF = the formation factor of the rock corrected for clay conductivity, C_w = the conductivity of the pore fluid, B = the equivalent conductance of the sodium ions absorbed onto the pore surfaces, Q_v = the CEC of the rock per unit pore volume, μ^2 = a dimensionless number meant to compensate for the tortuosity of the pore surfaces with respect to that of the pore space, and C_o = the conductivity of the fluid-bearing rock.

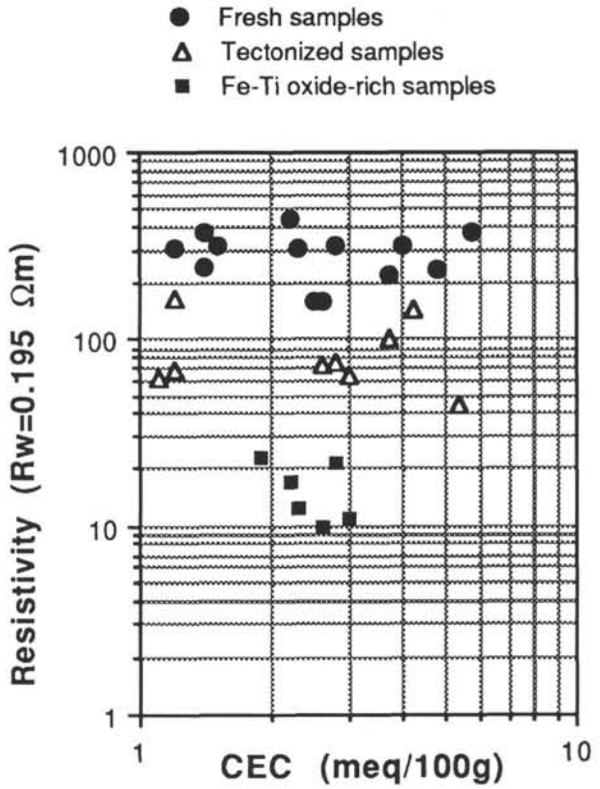

Figure 5. CEC vs. resistivity (at seawater salinity).

As boundary conditions for this model, values of μ equal to 1.0 or 100.0, respectively, would provide values of ($B \cdot Q_v/\mu^2$) either too large or too small to be significant. A value of μ = 10.0 thus was chosen to model the surface conduction. Figure 6 shows that surface conduction contributes little, if at all, to the overall electrical conduction during *in-situ* measurements, as C_w equals about 5000.0 $m\Omega^{-1}\,m^{-1}$, compared to ($B \cdot Q_v/\mu^2$), which is of the order of 25.0 $m\Omega^{-1}\,m^{-1}$ for $\mu = 10.0$. For the few anomalous samples from the upper part of Hole 735B with low CEC values (Units I and II), the contribution of surface conduction is even smaller.

Electrical Conduction in Gabbros

The two resistivity-porosity crossplots in Figure 7 show that fresh and tectonized samples can be related by a regression similar to that of Winsauer and McCardell (1953). However, the oxide-rich samples do not follow the same line. This suggests the existence of at least two dominant mechanisms for electrical conduction in the rocks recovered from Hole 735B. Figures 8 and 9 summarize the conductivities measured at four different saturating-fluid salinities. Whereas no consistent rule results from the grouping of samples based on the lithostratigraphic zonation (Fig. 8), similar relationships do appear when grouping is based on fresh, altered, and oxide-rich samples (Fig. 9).

As expected, fresh samples are the most resistive and oxide-rich samples the most conductive. However, it appears that (1) surface conduction contributes little to the conductivity of the samples at seawater salinity in the case of fresh or tectonized samples and (2) both surface and electrolytic conductions can be ignored at seawater salinity ($C_w = 5.0\ \Omega^{-1}\ m^{-1}$) for Fe-Ti oxide-rich samples. These two points might be illustrated as follows. At seawater salinity ($C_w = 5.0\ \Omega^{-1}\ m^{-1}$), the sample conductivity increases with fluid salinity (or con-

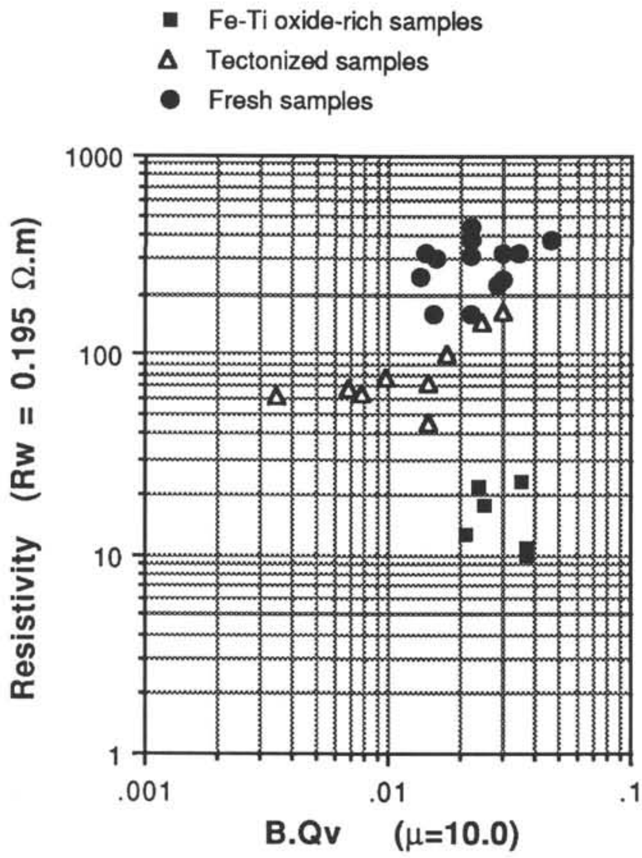

Figure 6. Surface conductivity vs. resistivity (at seawater salinity).

ductivity) for fresh and tectonized samples, thereby proving that the main conduction mechanism in this salinity domain is electrolytic (Pezard, in press). For Fe-Ti oxide-rich samples, the rock conductivity is near-constant at seawater conductivity ($C_w = 5.0\ \Omega^{-1}\ \mathrm{m}^{-1}$), and the main conduction mechanism then is attributed to the high concentration of metallic oxides in the matrix. As a consequence, the conduction of electrical current for the gabbros recovered in Hole 735B can be described by a model of electrical conduction in parallel:

$$C_o = (C_w/\mathrm{FF}) + C_{\mathrm{oxides}},$$

where C_{oxides} is the conduction component from the presence of metallic oxides in the matrix. Each of the 29 samples will be analyzed in the future for oxide content to study the potential relationship of C_{oxides} to oxide concentration.

Porosity and Formation Factor

The study is now restricted to nonoxide-bearing samples, where one can assume that C_{oxides} is negligible. The relationship observed in Figure 7 (at R_w = 1.02 ohm-m) is valid for each saturating-fluid salinity (Fig. 10), both for fresh (Fig. 11) and tectonized samples (Fig. 12). In both cases, the best fit is obtained with the most saline saturating-fluids. An average of the results obtained for the two most saline fluids (including seawater for R_w = 0.195 ohm-m) has been computed, and the following regression provides a means of estimating porosity from resistivity:

$$\mathrm{FF} = C_w/C_o = (8.04) \times \phi^{-1.08}.$$

This result is similar to that derived for MORB from DSDP Hole 418A (Broglia and Moos, 1988) and Hole 504B (Pezard, in press), subaerial basalts from Iceland (Flovenz et al., 1985), or even granites (Pape et al., 1985). The low *m* value (near 1.0) implies that the structure of the pore space of gabbros from Hole 735B is constituted of large aspect-ratio cracks and microcracks pervasively interconnected at the microscopic scale (e.g., Keller and Frischknecht, 1966; Shankland, 1975; Schwartz and Kimminau, 1988).

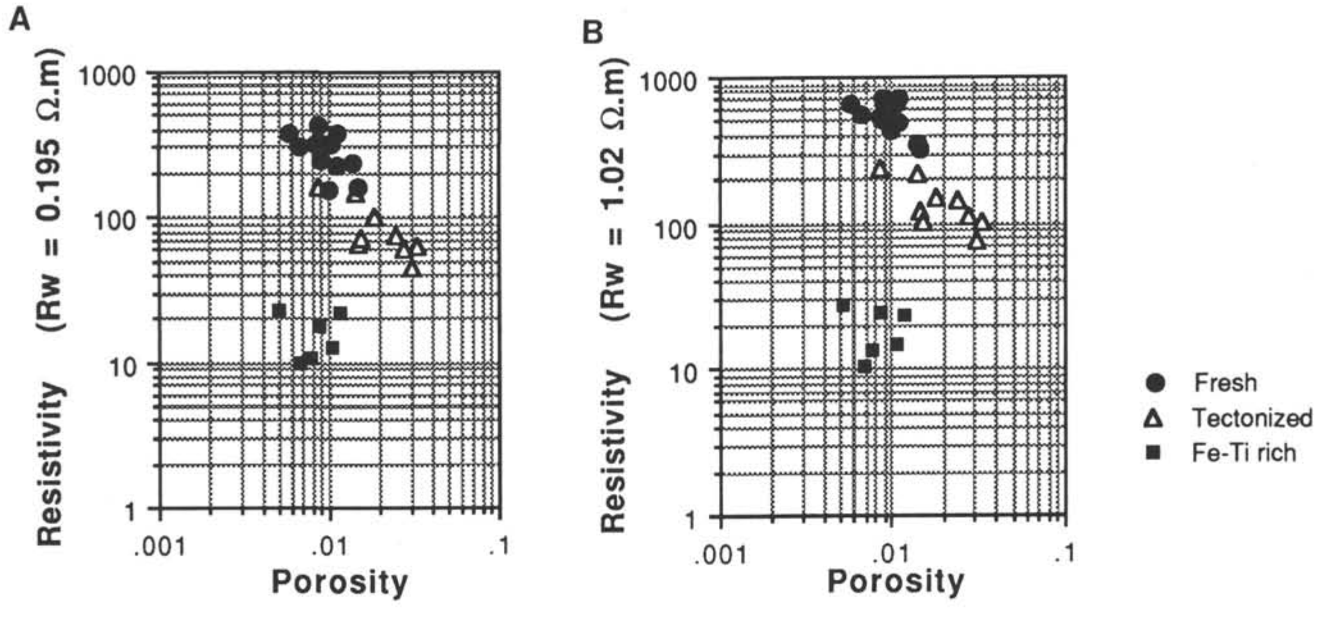

Figure 7. Porosity vs. resistivity at two saturating-fluid salinities: **(A)** seawater (R_w = 0.195 ohm-m) and **(B)** R_w = 1.02 ohm-m.

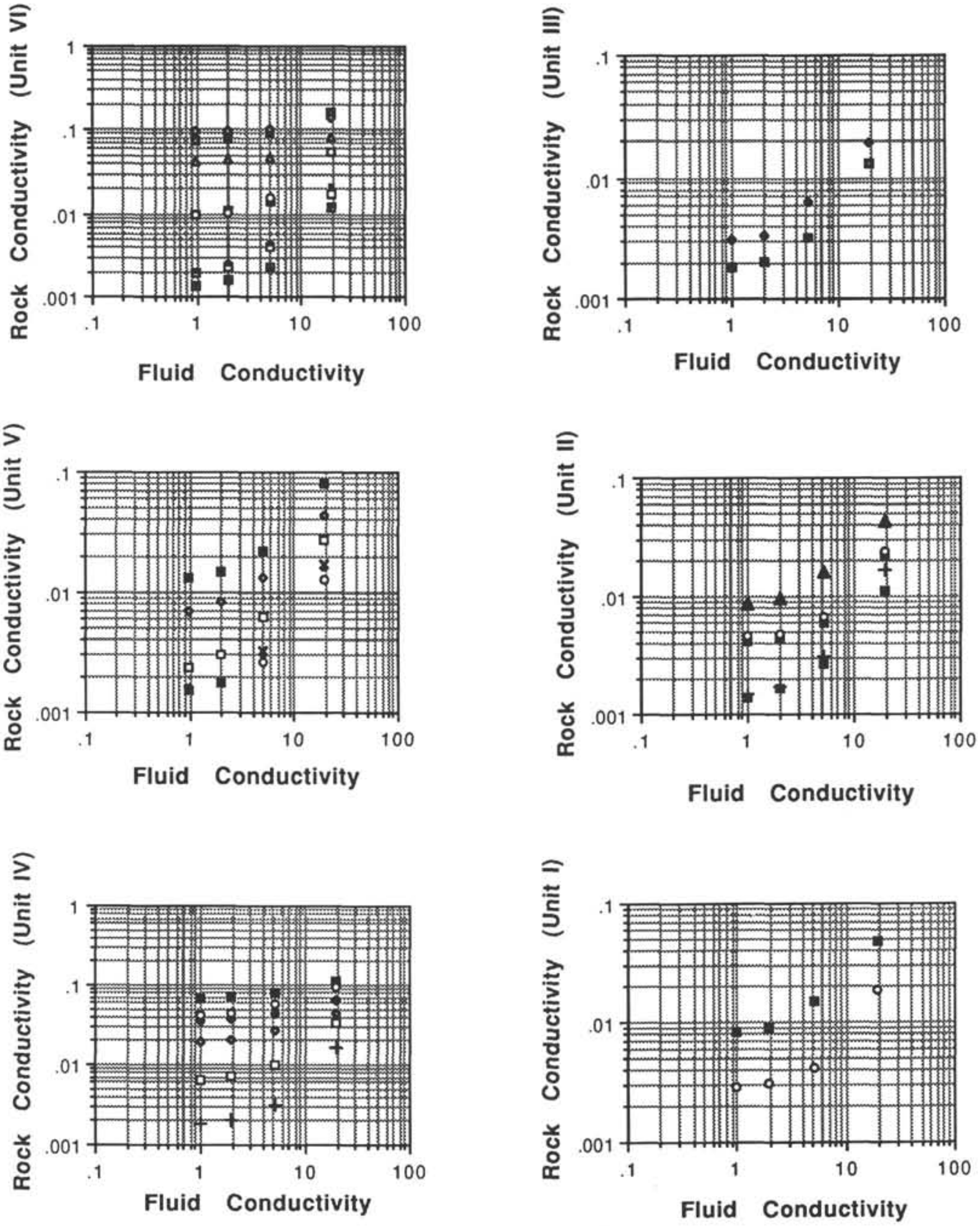

Figure 8. Electrical conductivity at four saturating-fluid salinities classified per lithologic units.

CONCLUSIONS

Surface conduction mechanisms can be ignored when analyzing downhole measurements of electrical resistivity recorded in gabbros at Site 735. The main conduction mechanisms for electrical current consequently are reduced to (1) electrolytic conduction in the pore space and (2) electronic conduction in metallic grains of the matrix because of the presence of Fe-Ti oxides. When a high oxide concentration is present, matrix conduction becomes the dominant conduction mechanism. This explains the low resistivity values recorded *in situ* with the dual laterolog in lithologic Unit IV and the lower part of the hole. The low *m* value obtained when relating porosity to formation factor suggests that the conducting pore space of gabbros is similar to that of MORB, that is, mainly composed of cracks and microcracks, as observed elsewhere in thin sections.

ACKNOWLEDGMENTS

We thank the co-chiefs, Paul Robinson and Richard Von Herzen, for allowing us to sample the rocks recovered during Leg 118; Janice Gittings for her assistance at various stages of this study; Michael Lovell, Mathilde Cannat, and Henriette Lapierre for helping to shape a better manuscript through informal discussions; and Morton Ridge and Larry McGowan of Schlumberger-Doll Research for providing their help with laboratory measurements. This study was supported by the NSF through a JOI/USSAC grant administered by the Texas A&M Research Foundation.

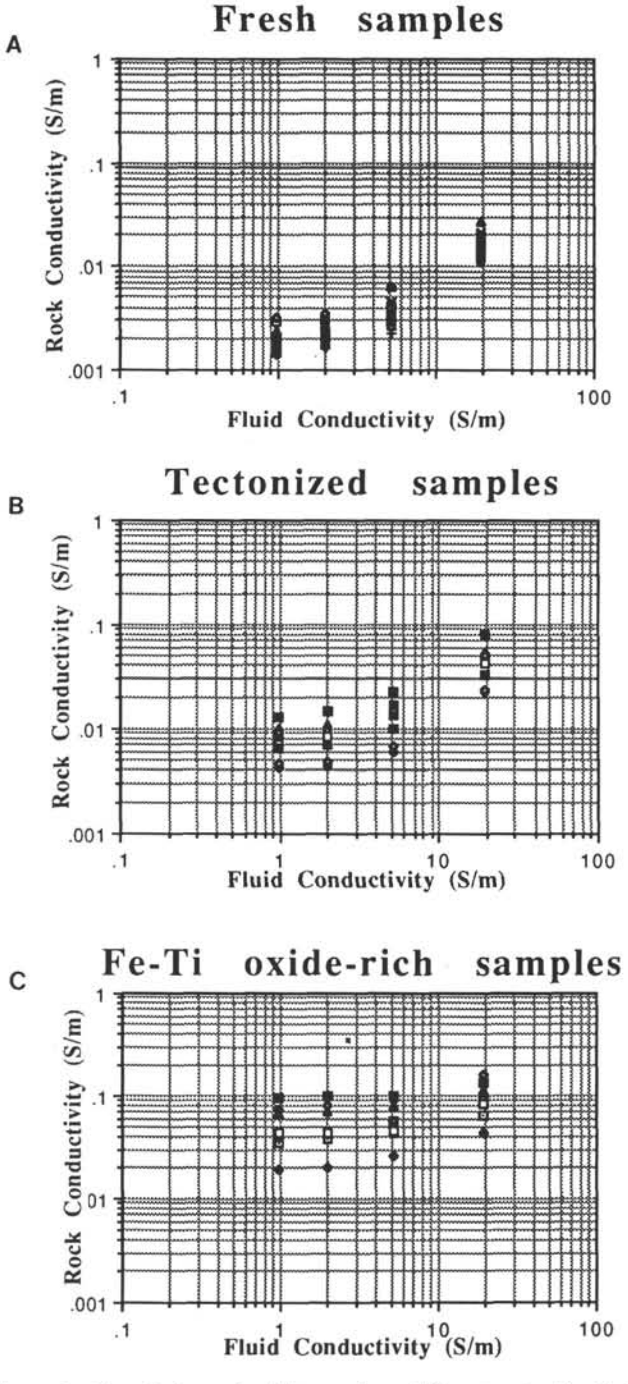

Figure 9. Electrical conductivity at four different saturating-fluid salinities of samples classified in three arbitrary categories: **(A)** fresh, **(B)** tectonized, and **(C)** Fe-Ti oxide-rich samples.

REFERENCES

Anderson, R. N., Honnorez, J., Becker, K., et al., 1985. *Init. Repts. DSDP*, 83: Washington (U.S. Govt. Printing Office).

Archie, G. E., 1942. The electrical resistivity log as an aid in determining some reservoir characteristics. *J. Pet. Technol.*, 5:1–8.

Becker, K., Sakai, H., et al., 1988. Site 504. *Proc. ODP, Init. Repts.*, 111: College Station, TX (Ocean Drilling Program).

Boillot, G., Winterer, E. L., et al., 1987. Site 637. *Proc. ODP, Init. Repts.*, 103: College Station, TX (Ocean Drilling Program).

Brace, W. F., Orange, A. S., and Madden, T. R., 1965. The effect of pressure on the electrical resistivity of water-saturated crystalline rocks. *J. Geophys. Res.*, 70:5669–5678.

Broglia, C., and Moos, D., 1988. *In situ* structure and properties of 110 Ma crust from geophysical logs in DSDP Hole 418A. *In* Salisbury, M. H., Scott, J., et al., *Proc. ODP, Sci. Results*, 102: College Station, TX (Ocean Drilling Program), 29–47.

Clavier, C., Coates, G., and Dumanoir, J., 1977. The theoretical and experimental bases for the dual-water model for the interpretation of shaly sands. Pap. 6859 presented at the *Soc. Pet. Engrs. 52nd Annu. Tech. Conf.* (Denver).

Donnelly, T., Francheteau, J., et al., 1979. *Inits. Repts. DSDP*, 51, 52, 53: Washington (U.S. Govt. Printing Office).

Drury, M. J., and Hyndman, R. D., 1979. The electrical resistivity of oceanic basalts, *J. Geophys. Res.*, 84:4537–4546.

Ellis, D. V., 1987. *Well Logging for Earth Scientists:* New York (Elsevier).

Flovenz, O. G., Georgsson, L. S., and Arnasson, K., 1985. Resistivity structure of the upper crust in Iceland. *J. Geophys. Res.*, 90:10136–10150.

Keller, G. V., and Frischknecht, F. C., 1966. *Electrical Methods in Geophysical Prospecting:* Oxford (Pergamon Press).

Olhoeft, G. R., 1981. Electrical properties of rocks. *In* Touloukian, Y. S., Judd, W. R., and Roy, R. F. (Eds.), *Physical Properties of Rocks and Minerals*: New York (McGraw-Hill), 257–330.

Pape, H., Riepe, L., and Schopper, J. R., 1985. Petrophysical detection of microfissures in granites. *SPWLA 26th Annu. Logging Symp.* (Dallas), Pap. P.

Pezard, P. A., in press. Electrical properties of MORB and implications for the structure of the upper oceanic crust at Site 504. *J. Geophys. Res.*

Rai, C. S., and Manghnani, M. H., 1981. The effect of saturant salinity and pressure on the electrical resistivity of Hawaiian basalts. *Geophys. J. Roy. Astron. Soc.*, 65:395–405.

Ridge, M. J., 1983. A combustion method for measuring the cation exchange capacity of clay minerals. *Log Analyst*, 3:6–11.

Robinson, P. T., Von Herzen, R. P., et al., 1989. Site 735. *Proc. ODP, Init. Repts.*, 118: College Station, TX (Ocean Drilling Program).

Schwartz, L. M., and Kimminau, S., 1987. Analysis of electrical conduction in the grain consolidation model. *Geophysics*, 52:1402–1411.

Serra, O., 1984. *Fundamentals of Well-Log Interpretation:* Amsterdam (Elsevier).

Shankland, T. J., 1975. Electrical conduction in rocks and minerals: parameters for interpretation. *Phys. Earth Planet. Int.*, 10:209–219.

Waxman, M. H., and Smits, L.J.M., 1968. Electrical conductivities in oil-bearing shaly sands. *Pet. Trans. AIME*, 243:240–248.

Winsauer, W. O., and McCardell, W. M., 1953. Ionic double-layer conductivity in reservoir rocks. *Pet. Trans. AIME*, 198:129–134.

Wyllie, R. J., and Gregory, A. R., 1953. Formation factors of unconsolidated porous media: influence of particle shape and effects of cementation. *Pet. Trans. AIME*, 198:103–110.

Date of initial receipt: 12 July 1989
Date of acceptance: 4 June 1990
Ms 118B-161

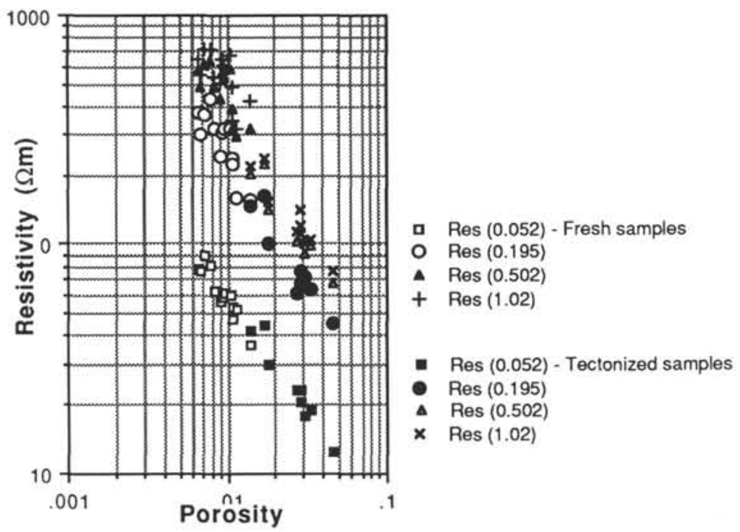

Figure 10. Porosity vs. resistivity for fresh and tectonized samples.

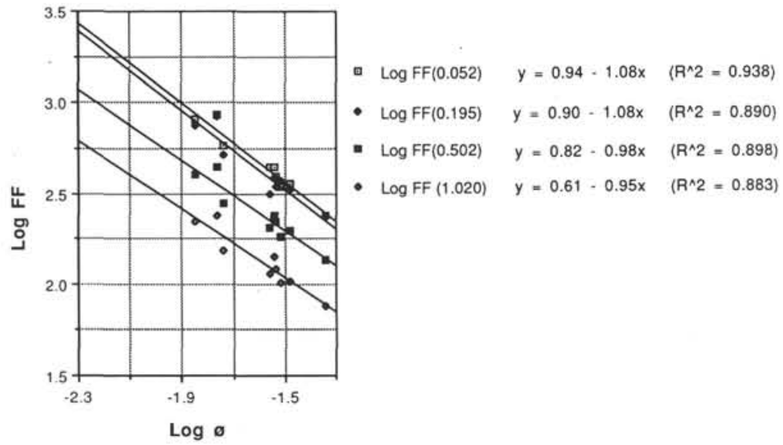

Figure 11. Regressions obtained for formation factor vs. porosity at four different fluid salinities for fresh samples.

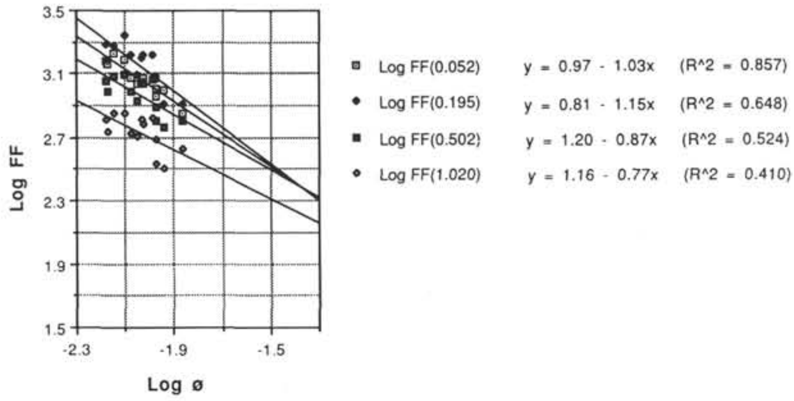

Figure 12. Regressions obtained for formation factor vs. porosity at four different fluid salinities for tectonized samples.